

Application of the method of caustics to the centre-cracked diametral compression test specimen

D. SINGH, D. K. SHETTY

Department of Materials Science and Engineering, University of Utah, Salt Lake City, Utah 84112, USA

Normalized Mode I stress intensity factors, $N_I(a/R)$, for symmetrical radial cracks in diametral compression test specimens were experimentally evaluated using disc specimens of polymethyl methacrylate and the method of caustics. The method of caustics was first employed with precracked three-point bend specimens to assess the optical constant for the test material. This material property and the diameters of the caustics as a function of the applied load at different relative crack lengths (a/R) yielded the non-dimensional stress intensity factors using equations presented by Theocaris. These experimental values agreed closely with the theoretical solutions reported in the literature. Disc specimens of a polycrystalline alumina were also tested in diametral compression at temperatures up to 1000°C and the measured fracture toughness values were compared to those measured with chevron-notched bend specimens. It is shown that the centre-cracked diametral compression specimens give very reproducible fracture toughness measurements, and the specimen and the test technique can be usefully employed to assess the fracture toughness of structural ceramics at both ambient and elevated temperatures.

1. Introduction

The diametral compression test in which a disc specimen is loaded in compression along a diameter is used quite extensively to measure the strengths of such materials as rocks, cement, concrete and ceramics with moderate strengths. A tensile stress that develops normal to the plane of loading and splits the disc specimen along the loading diameter is used to assess an "indirect" tensile strength. Fracture statistics and mechanics analyses are then used to correlate this strength with other common measures of strength, for example the modulus of rupture assessed in three- or four-point bend tests [1, 2].

The diametral compression test specimen can also be used for measuring the fracture toughness of brittle materials by introducing radially symmetric through-cracks in the disc specimens. Yarema and Krestin [3] used notched disc specimens to measure Mode I fracture toughness of concrete, while Libatskii and Krestin [4] measured the Mode I fracture toughness of organic and inorganic glasses using this test geometry. Subsequently, Awaji and Sato [5] and Yarema *et al.* [6] used the disc specimens to measure combined-mode (Mode I and Mode II) fracture toughness of brittle materials by aligning the central notch at an angle to the loading diameter. In all of the above studies, machined notches were used instead of "sharp" cracks. Shetty *et al.* [7, 8] used chevron notches to precrack the disc specimens prior to testing in pure Mode I, pure Mode II or combined Mode I and Mode II loading. It is well known that notched specimens generally overestimate

Mode I fracture toughness if the notch opening is greater than a material characteristic value [9]. In predominantly Mode II loading, however, precracked specimens tend to give higher fracture toughness than the notched specimens in polycrystalline materials. This is due to crack surface resistance to Mode II displacement in precracked specimens because of the interlocking effect of asperities at the microstructural level [10].

The centre-cracked diametral compression test specimen is particularly attractive for use with advanced structural ceramics. The compressive mode of loading is relatively easy to implement at high temperatures of interest with ceramics. Ceramic disc specimens are easily fabricated by such conventional methods as hot pressing or cold pressing and sintering and the discs require minimal machining after fabrication. There is also a growing interest in the mixed-mode fracture behaviour of structural ceramics to establish a realistic fracture criterion for use in design.

Solutions for stress intensity factors for symmetric centre cracks in diametral compression specimens have been reported by Yarema and co-workers [3, 4, 6], Awaji and Sato [5] and, more recently, Atkinson *et al.* [11]. These solutions are in good agreement with each other, despite the different analytical and/or numerical procedures that were used in obtaining these solutions. However, there has been no independent experimental verification of these theoretical results. The present paper reports the results of an experimental investigation of stress intensity factors

TABLE I Dimensions of diametral compression and chevron bend specimens of PMMA and alumina

Material	R (mm)	R_1 (mm)	S (mm)	W (mm)	B (mm)	a_0 (mm)	a_1 (mm)	N (μm)
<i>Diametral compression specimens</i>								
PMMA	50.8	19.1			6.4	2.4	10.8	250
Alumina	15.9	11.1			2.5	3.9	6.4	200
<i>Chevron bend specimens</i>								
Alumina and PMMA			40	10	6.7	3.3	9.1	200

for centre-cracked diametral compression specimens. The method of caustics developed by Theocaris [12–14] was used with precracked specimens of polymethyl methacrylate (PMMA). The experimentally assessed non-dimensional stress intensity factors, $N_1(a/R)$, in the normalized crack length range $a/R = 0.1$ to 0.5 , are shown to be in good agreement with the theoretical solutions. The diametral compression test was also used to characterize the Mode I fracture toughness of a polycrystalline alumina at temperatures up to 1000°C . The measured fracture toughness values are in good agreement with those measured using chevron-notched, three-point bend test specimens.

2. Experimental procedures

2.1. Materials and test specimens

PMMA and a commercial-grade polycrystalline alumina (Greenleaf Technical Ceramics, Hayward, California) were used in the present study. PMMA was used because it is a model brittle material, well suited for the method of caustics because of its isotropic elastic and optical properties and low elastic modulus. The polycrystalline alumina was used as a representative structural ceramic for investigating application of the diametral compression test for evaluating fracture toughness at elevated temperatures. The microstructure of the alumina consisted of 89 vol % Al_2O_3 with an average grain size of $21\ \mu\text{m}$ and a remaining glassy phase of unknown composition. Young's modulus (E) and Poisson's ratio (ν) for the alumina measured by using strain gauges on an uncracked diametral compression test specimen, as discussed by Hondros [15], were 421 GPa and 0.29, respectively.

Fig. 1 shows the geometry of the diametral compression test specimens used in this study. The dimensions of the specimens of the two materials are listed in Table I. Symmetric chevron notches were machined in the centre of the disc specimens using either steel cutting blades for PMMA or diamond grit blades for

the alumina. The PMMA disc specimens for the caustics measurements were precracked to desired lengths by compression-loading the discs in the plane of the notch. The Mode I stress intensity factor, K_I , for a crack in a disc specimen loaded in the plane of the crack is given by the following equation [11]:

$$K_I = \frac{P(\pi a)^{1/2}}{\pi RB} N_1 \quad (1)$$

where P = load applied to the disc in diametral compression, R = radius of the disc specimen, B = thickness of the disc specimen, a = radial crack length ($a > a_1$ in Fig. 1), and N_1 = a non-dimensional coefficient of Mode I stress intensity factor dependent on the relative crack length (a/R).

Atkinson *et al.* [11] have reported solutions for N_1 for cracks of length up to $a/R = 0.6$. Their results can be accurately fitted by the following cubic polynomial:

$$N_1 = 0.991 + 0.141 \left(\frac{a}{R}\right) + 0.863 \left(\frac{a}{R}\right)^2 + 0.886 \left(\frac{a}{R}\right)^3 \quad (2)$$

In addition to the disc specimens, chevron-notched three-point bend specimens of the geometry shown in Fig. 2 were also used in this investigation. The dimensions of these specimens are also listed in Table I. The three-point bend specimens of PMMA were used to independently establish the optical constant used in the analysis of the caustics data. All the three-point bend specimens of PMMA were stably precracked to the base of the chevron notch before using them in the caustics experiments. The precracked three-point bend specimen was used because the Mode I stress intensity factor for this specimen geometry is well established for wide ranges of crack length and is given by the following equation [16–18]

$$K_I = \frac{PS}{BW^{3/2}} f(\alpha) \quad (3)$$

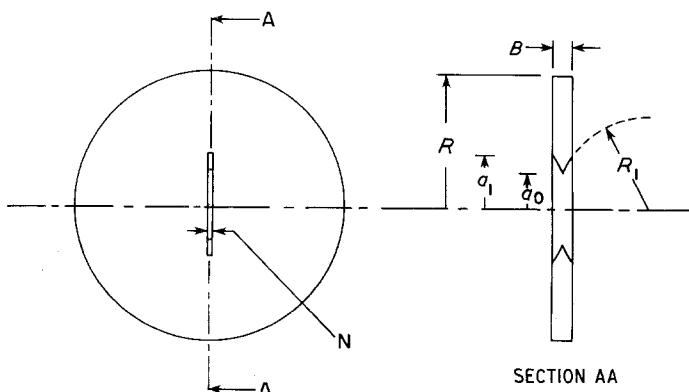


Figure 1 Geometry of the chevron-notched diametral compression specimens used in caustics experiments and fracture toughness measurements. N = notch opening.

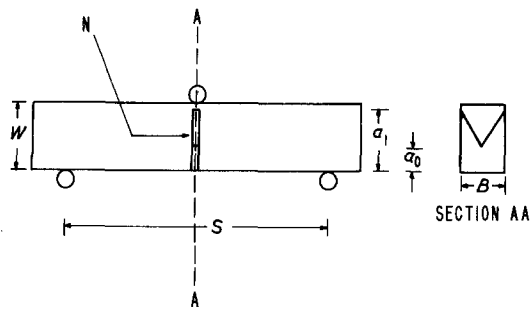


Figure 2 Geometry of the chevron-notched bend specimens used in the caustics experiments and fracture toughness measurements. N = notch opening.

where P = load applied in bending, S = specimen support span, B = specimen thickness, W = beam height, α = normalized crack length (a/W), and $f(\alpha)$ is a non-dimensional coefficient of the stress intensity factor given by the equation

$$f(\alpha) = \frac{3\alpha^{1/2}[1.99 - \alpha(1 - \alpha)(2.15 - 3.93\alpha + 2.7\alpha^2)]}{2(1 + 2\alpha)(1 - \alpha)^{3/2}} \quad (4)$$

2.2. Method of caustics

Several experimental techniques are now available for evaluating stress intensity factors for cracked specimens under load. Recent discussions of these techniques can be found elsewhere [14, 16–18]. Theocaris [12–14] developed and extensively used an optical technique that was introduced by Manogg [19]. The technique, referred to as the method of caustics, has also been used by Seidelmann *et al.* [20] to determine critical mixed-mode stress intensity factors for inclined cracks in thin sheets of PMMA. In this technique, a monochromatic and coherent light beam from a laser is passed through the crack tip region of an optically isotropic and transparent brittle material such as PMMA as shown in the schematic diagram of Fig. 3. Due to the high stress concentration at the crack tip and the consequent thickness variation in a thin specimen under a plane state of stress the transmitted beam is locally deflected. A characteristic shadow spot surrounded by a bright caustic, as shown in Fig. 4, appears on a screen placed in the path of the transmitted beam. It has been shown by Theocaris and Gdoutos [13] that

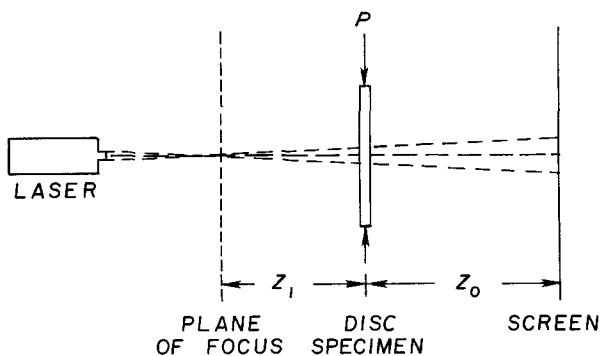


Figure 3 Schematic diagram of the experimental arrangement for measuring the transmitted caustics. Magnification factor $\lambda = (z_1 + z_0)/z_1$.

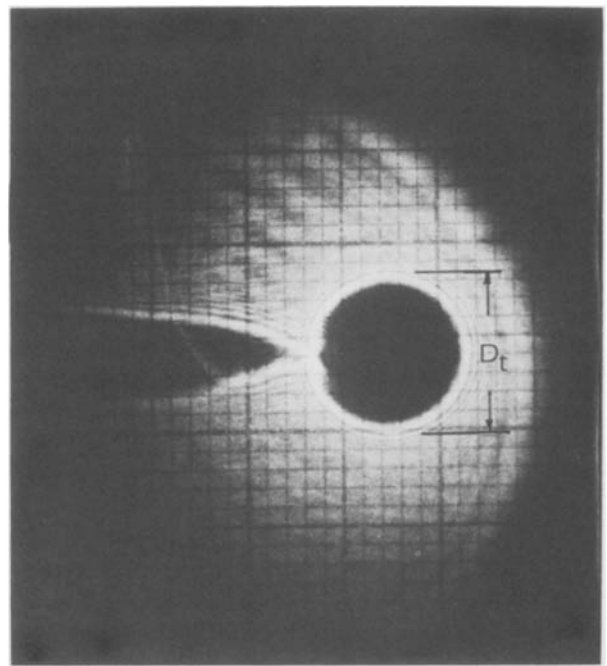


Figure 4 A typical transmitted caustic from a precracked disc specimen of PMMA subjected to Mode I loading.

the size and shape of the caustic are related to the stress intensity factors governing the local elastic deformation of the plate in the thickness direction, the thickness of the specimen (B), an optical constant for PMMA (c) and certain optical magnification factors. The following equation applies to test specimens subjected to pure Mode I loading:

$$K_I = \frac{(8\pi)^{1/2} D_t^{5/2}}{3z_0 B c \lambda^{3/2} \delta^{5/2}} \quad (5)$$

where z_0 = distance of the screen from the midplane of the specimen (Fig. 3), and D_t = diameter of the caustic in a plane perpendicular to the crack and going through the crack tip (see Fig. 4).

δ and λ in Equation 5 are two magnification factors. δ is the ratio of the transverse diameter (D_t) of the caustic and the radius of the circular envelope of the constrained zone at the specimen crack tip. For pure Mode I loading δ takes the value 3.16. λ is a magnification factor of the optical arrangement given by

$$\lambda = (z_0 + z_1)/z_1 \quad (6)$$

where z_1 is the distance of the plane of focus from the midplane of the specimen (see Fig. 3). In the experimental set-up used in this study z_0 was approximately 0.5 m and z_1 was in the range of 0.5 to 0.7 m. The transverse diameter of the caustic, D_t , was measured from a trace on the screen using vernier callipers.

2.3. Fracture toughness measurements

The fracture toughness of the polycrystalline alumina was evaluated at temperatures up to 1000°C using both the centre-cracked diametral compression specimens and the chevron-notched bend specimens. It has been shown by Shetty *et al.* [7] that on loading a chevron-notched disc specimen in diametral compression, sharp cracks initiate at the tips of the chevron notches; they extend stably through the chevron section

and they become unstable at the base of the chevron notch (i.e. when $a = a_1$ in Fig. 1). Fracture toughness is, therefore, calculated from Equation 1 with $P = P_f$, the fracture load, and $a = a_1$. In the chevron-notched bend specimens, on the other hand, fracture instability occurs for a crack length in the chevron section. This critical crack length and the corresponding critical stress intensity factor for the chevron-notched bend specimens can be calculated by using either the assumption of the equivalent straight-through crack (STCA) or using a slice synthesis model for the compliance [21–23]. The critical stress intensity factor is expressed in the form

$$K_{Ic} = \frac{P_f S}{BW^{3/2}} Y_m \quad (7)$$

where Y_m is a non-dimensional parameter. In the STCA analysis, Y_m is given by the minimum value of the non-dimensional compliance function

$$Y = f(\alpha) \left(\frac{\alpha_1 - \alpha_0}{\alpha - \alpha_0} \right)^{1/2} \quad (8)$$

where α_0 , α and α_1 are crack lengths a_0 , a and a_1 normalized with respect to W . Equations 7 and 8 were used to calculate fracture toughness from the fracture loads and the specimen and notch geometry of the bend specimens.

3. Experimental results

3.1. Method of caustics: three-point bend specimens

The method of caustics was first used with the pre-cracked three-point bend specimens of PMMA. Fig. 5 shows plots of the transverse diameter of the caustic

(D_t) as a function of the applied load (P) for normalized crack lengths (a/W) of 0.4 and 0.53. The straight lines in the log–log plots have a slope of 0.4 and the good fits to the data are consistent with Equation 5. A constant A , corresponding to the intercepts of the log–log plots, was defined by the equation

$$D_t = AP^{2/5} \quad (9)$$

The constant A is related to the non-dimensional stress intensity factor, $f(\alpha)$, via the specimen dimensions and the geometrical and the optical magnification factors (z_0 , λ and δ) and the optical constant c via Equations 3 and 5. The equation applicable to the bend specimens is

$$f(\alpha) = \frac{A^{5/2} W^{3/2} (8\pi)^{1/2}}{3S z_0 c \lambda^{3/2} \delta^{5/2}} \quad (10)$$

Theocaris [12, 13] has used a value $c = 1.071 \times 10^{-10} \text{ m}^2 \text{ N}^{-1}$ for PMMA. In Fig. 6 the values of $f(\alpha)$ calculated using this value of the optical constant c and the other applicable values of the constants in Equation 10 are plotted as a function of the normalized crack length, $\alpha = a/W$. Also shown in the figure is a plot of Equation 4 which is an empirical equation devised to fit those analytical results for this specimen geometry that were considered to be the most accurate and reliable [16–18]. The experimental values of $f(\alpha)$ are in good agreement with the analytical results. This agreement validates the method of caustics and the applicable equations for assessing the non-dimensional stress intensity factor, $f(\alpha)$. Conversely, the agreement can be viewed as confirming the value of the optical constant c for the PMMA used in this study.

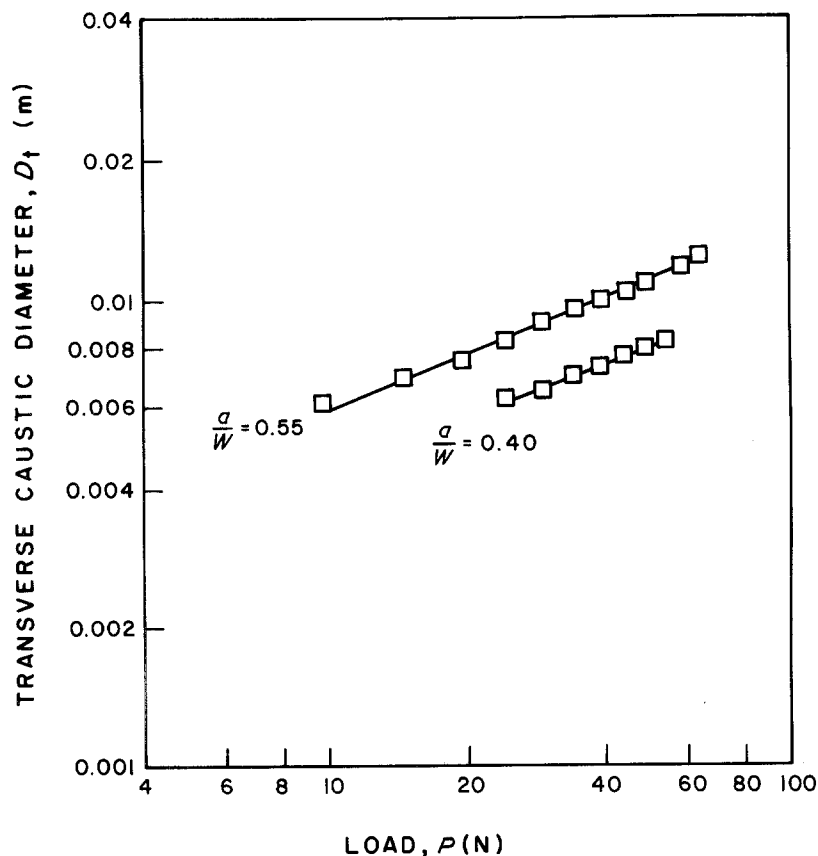


Figure 5 Transverse diameter of the caustic (D_t) against bending load (P) for pre-cracked three-point bend specimens of PMMA.

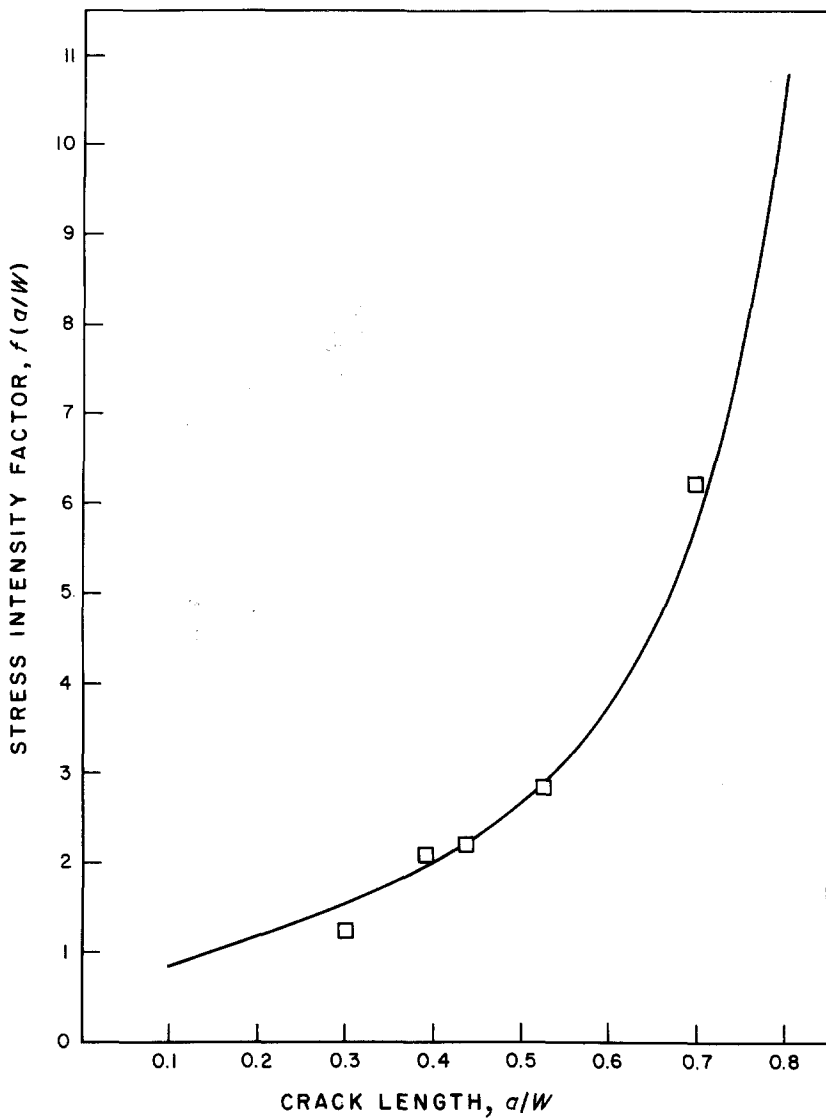


Figure 6 Non-dimensional stress intensity factor, $f(a)$, for precracked three-point bend specimens. (\square) method of caustics, (—) from Srawley [16].

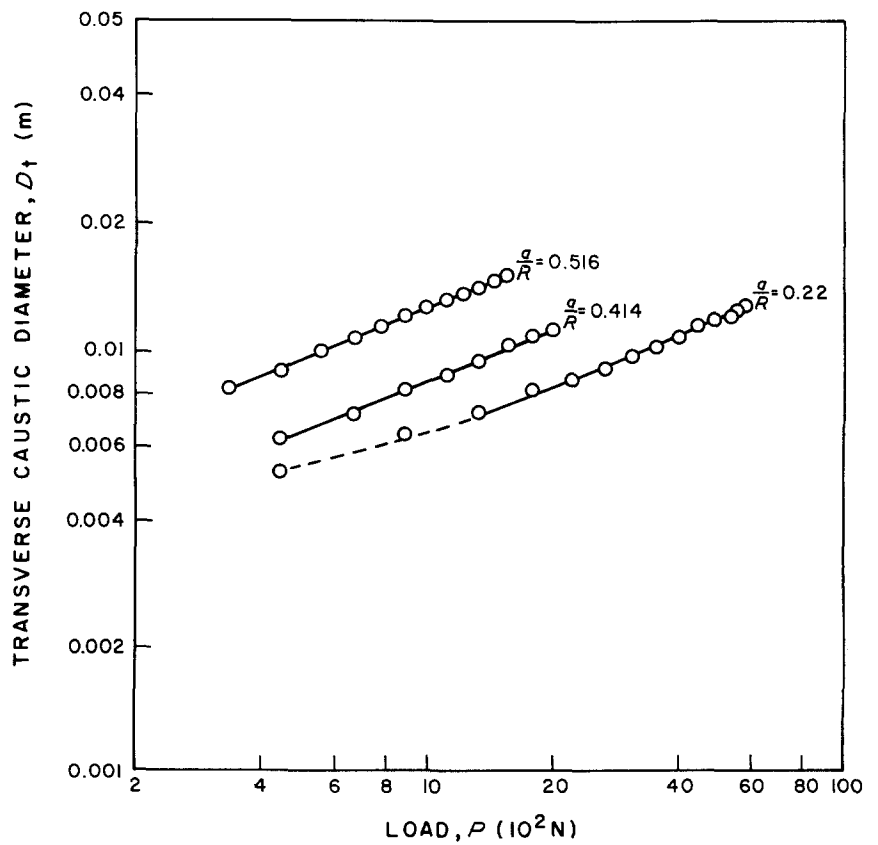


Figure 7 Transverse diameters of the caustics (D_t) against load in compression (P) for precracked diametral compression specimens of PMMA.

3.2. Method of caustics: diametral compression specimens

Fig. 7 shows three log-log plots of the transverse diameters of the caustics as a function of the load applied in diametral compression for disc specimens with relative crack lengths of 0.22, 0.414 and 0.516. The solid lines fitted to the data are again straight lines of slope 0.4. Caustics on disc specimens with large cracks showed good agreement with this expected slope. In disc specimens with relatively short cracks, however, caustics at small loads showed a systematic deviation to lower slopes. The reason for this deviation, which is indicated by the dashed line in Fig. 7, is not clear. In these cases, only the data at high loads that corresponded to the slope of 0.4 were used to calculate the intercept and the non-dimensional stress intensity factor N_I using the following equation:

$$N_I(a/R) = \frac{A^{5/2} \pi R (8\pi)^{1/2}}{3(\pi a)^{1/2} z_0 c \lambda^{3/2} \delta^{5/2}} \quad (11)$$

Fig. 8 shows a comparison of the values of $N_I(a/R)$ calculated from the above equation and the solution of Atkinson *et al.* [11] represented by the polynomial of Equation 2. Again, the agreement between the analytical solution and the method of caustics is quite good.

3.3. Fracture toughness of polycrystalline alumina

Fig. 9 summarizes fracture toughness data for the polycrystalline alumina at room temperature (25°C) and elevated temperatures up to 1000°C. The data plotted are the mean values of measurements on three

or more specimens and the error bars represent two standard deviations. The diametral compression test specimens gave exceptionally low scatter, particularly at elevated temperatures. As a result, no error bars are indicated for the high-temperature diametral compression measurements. At room temperature, the fracture toughness measured with the diametral compression test specimens ($K_{Ic} = 4.03 \pm 0.14 \text{ MPa m}^{1/2}$) is about 16% lower than the value measured with the chevron bend specimens ($K_{Ic} = 4.8 \pm 0.3 \text{ MPa m}^{1/2}$). This trend is similar to that observed by Shetty *et al.* [7] on soda-lime glass, a glass-ceramic and a polycrystalline alumina. In all these three ceramics, the diametral compression tests gave lower fracture toughness as compared to other techniques.

In both the diametral compression tests and the chevron bend tests, the fracture toughness of the alumina increased with temperature to a peak value at an intermediate temperature ($\sim 700^\circ\text{C}$) and then decreased sharply above 800°C . The fracture toughness measured with the chevron bend tests were consistently higher at room temperature and at 700°C , i.e. in the range where fracture toughness increased with temperature. At 800°C and high temperatures, however, there was no apparent difference in the measured values of the two tests.

Pabst *et al.* [24] have measured the fracture toughness of different grades of alumina at temperatures up to 1400°C . Their results indicate that alumina ceramics with significant amounts of glassy phase exhibit maxima in fracture toughness at intermediate temperatures ($\sim 900^\circ\text{C}$) and a sharp decrease at higher temperatures. These same grades of the alumina ceramics also

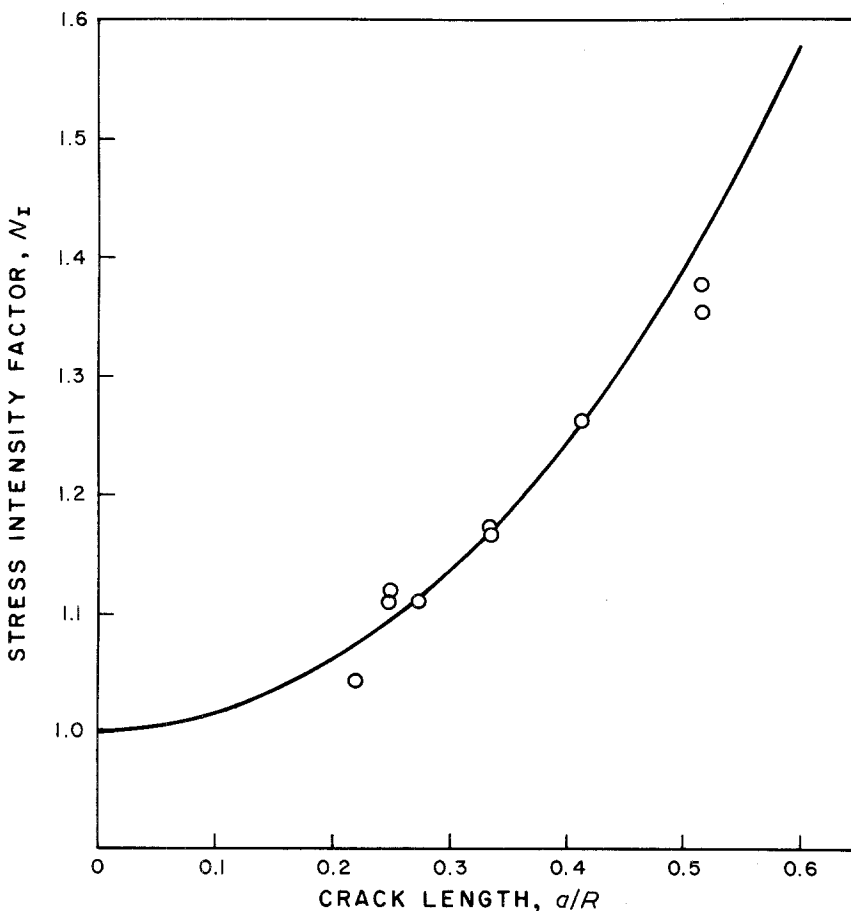


Figure 8 Non-dimensional Mode I stress intensity factor for symmetrical radial cracks in diametral compression specimens: (O) Method of caustics, (—) from Atkinson *et al.* [11].

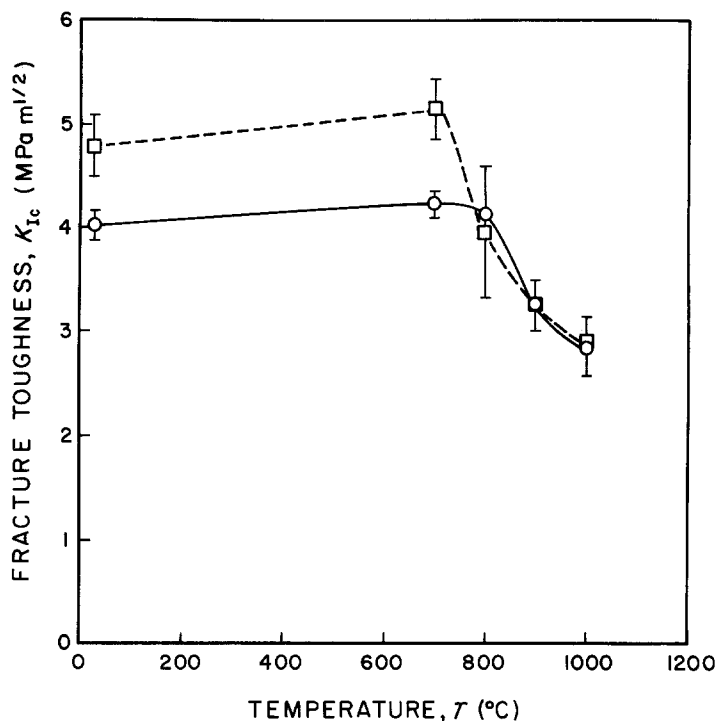


Figure 9 Temperature dependence of fracture toughness of alumina. (○) Diametral compression, (□) chevron bend.

exhibited a strong dependence of the fracture toughness on loading rate at elevated temperatures [24]. To see if the alumina used in this study had similar characteristics, diametral compression tests were conducted at 1000°C as a function of the machine crosshead speed. The results are shown in Fig. 10. The fracture toughness showed only a very modest increase with increasing crosshead speed; an increase of the crosshead speed from 0.002 to 0.08 mm sec⁻¹ increased the fracture toughness from 2.82 to 3.0 MPa m^{1/2}. The significant decrease of the fracture toughness at 1000°C relative to the fracture toughness at room temperature must be primarily due to other factors.

4. Discussion

The primary objective of this study was to use the method of caustics to evaluate Mode I stress intensity factors for symmetrical radial cracks in diametral compression specimens and compare the experimental results to analytical solutions. The method of caustics is attractive for experimental evaluation of stress intensity factors because the experimental procedure and the analyses of the results are relatively simple and the extensive work conducted by Theocaris [12–14] using this technique has shown that accurate results can be obtained by this method. It is clear from Equation 5 that the accuracy of the measured stress

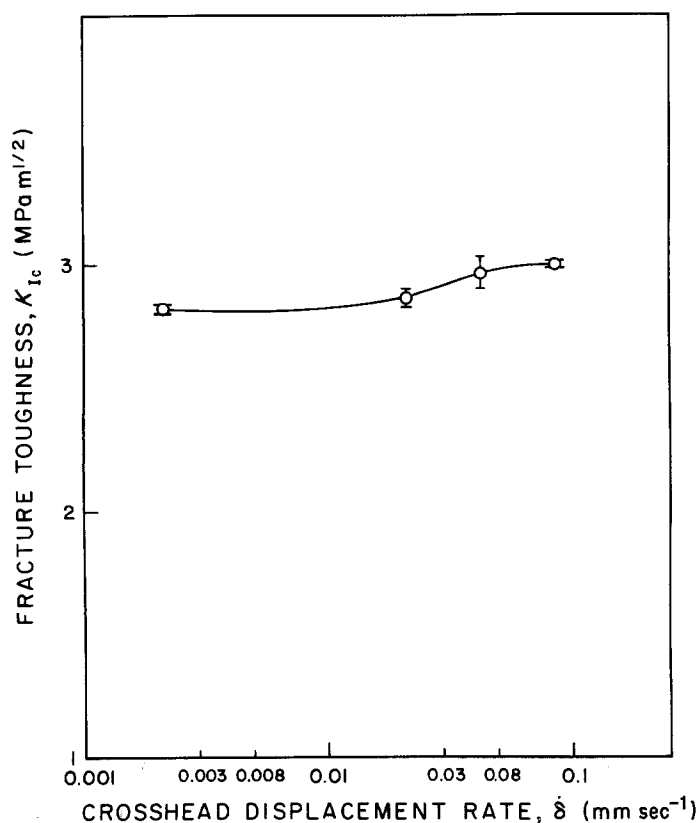


Figure 10 (○) Variation of fracture toughness of alumina with crosshead speed (diametral compression).

intensity factor is largely determined by the errors in the measurements of the caustic diameter (D_c) and the magnification factor, λ . The caustic diameters in this study were measured to an accuracy of 0.5 mm and this limited the accuracy of the measured stress intensity factors, especially for small loads. In view of this limitation, the agreement obtained between the analytical and/or the numerical solutions and the experimentally measured stress intensity factors for both the bend specimens and the disc specimens is considered very good. Improved techniques for measuring the caustic diameters, such as, for example, the photomultiplier tube and oscilloscope used by Sukere [25] in his recent study, and increased optical magnification factor (λ) to increase the absolute sizes of the caustics are currently being investigated to increase the overall accuracy of the method of caustics.

The experimental measurements of stress intensity factors for the diametral compression specimens in this study covered normalized crack lengths (a/R) ranging from about 0.2 to 0.5. In this range, there is no systematic deviation of the measured stress intensity factors from the analytical solution of Atkinson *et al.* [11]. This result and the fact that the solution of Atkinson *et al.* agrees with other analytical solutions, for example the solution recently given by Yarema *et al.* [6], can be taken as evidence of the accuracy of the stress intensity factor relation used in calculating fracture toughness from the diametral compression test results. As the crack length increases and the crack tips approach the loading points, however, the solutions must break down since the stress intensity factor should then be sensitive to the local distribution of the load at the loading points. Atkinson *et al.* [11] have stated that their solutions are valid for relative crack lengths up to 0.6.

The fracture toughness of the alumina measured using the diametral compression tests showed two interesting characteristics. The values measured using the disc tests at room temperature and 700°C were significantly lower than those measured with the chevron bend tests. Similar observations have been made by Shetty *et al.* [7] on three other ceramics. These discrepancies are not likely to be due to any inaccuracies in the calculation of the stress intensity factors for reasons already discussed above. Secondly, the diametral compression tests gave exceptionally low scatter in the measured values.

It is believed that both of the above characteristics of the diametral compression test specimen are related to the one unique feature of the specimen and loading geometry, i.e. the presence of a high compressive stress parallel to the crack. Streit and Finnie [26] have demonstrated through experiments and analysis that a stress applied parallel to the crack has a strong influence on the crack path stability. The direction of the maximum hoop stress in the vicinity of a crack tip, for example, is influenced by this stress parallel to the crack. A compressive stress promotes in-plane crack growth, while a tensile stress promotes out-of-plane crack growth, through their influence on the local hoop stress. It is suggested that this crack path stability is also responsible for the low scatter in the measure-

ments of fracture toughness using the diametral compression tests.

Although the stress parallel to a crack has no effect on the stress intensity factor, it does affect the overall stresses and strains in the near-tip regions as discussed extensively by Liebowitz *et al.* [27]. Thus, fracture criteria formulated in terms of parameters other than the stress intensity factor, for example elastic strain energy release rate or local strain energy density, can be affected by the stress parallel to the crack. Eftis and Jones [28], for example, evaluated the influence of load biaxiality on the fracture load of centre-cracked sheets by calculating the elastic strain energy release rate using near-crack-tip stress and displacement relations that included second-order terms incorporating the effects of the remote stress parallel to the crack. Their calculations indicate that for such materials as ceramics, for which the Poisson's ratio is typically less than 0.33, the critical fracture load decreases with increasing remote compressive stress parallel to the crack. Biaxial fracture experiments on high-strength aluminium alloys, PMMA and other brittle polymers support the predictions of these calculations. The fracture toughness measurements with diametral compression specimens of the different ceramics are also qualitatively consistent with these predictions. This, however, does not explain why the two tests apparently give nearly identical fracture toughness values at high temperatures.

The temperature dependence of the fracture toughness of alumina observed in this study is similar to the trends observed by Pabst *et al.* [24] in different grades of alumina. In an alumina ceramic that contained 3% SiO₂, for example, fracture toughness showed a maximum at an intermediate temperature of 900°C and a sharp drop at higher temperatures. Both the intermediate maximum and the sharp decrease are believed to be related to the glassy phase in the alumina. However, the significant reduction in the fracture toughness at 1000°C relative to the room-temperature value in the alumina studied here (Fig. 9) cannot be all due to a subcritical crack growth mechanism related to the glassy phase. As seen in Fig. 10, the dependence of the fracture toughness at 1000°C on the machine crosshead speed is at best modest and accounts for only a fraction of the toughness difference between room temperature and 1000°C. The reduction in the fracture toughness must also be related to some other high-temperature reactions. Travitzky *et al.* [29] have shown that quenching of a commercial 85% Al₂O₃ ceramic from temperatures of about 1400°C increases the room-temperature fracture toughness by a factor of two in relation to the fracture toughness of a slowly cooled alumina. The toughness enhancement was attributed to compressive microstresses developed in the glassy phase. If such microstresses are present in the alumina in the as-received state, their annealing-out at high temperatures can contribute to the sharp decrease above 800°C noted in Fig. 9.

5. Conclusions

1. The method of caustics is a very viable experimental technique for experimentally assessing

stress intensity factors in fracture toughness specimens.

2. The normalized Mode I stress intensity factors for symmetrical radial cracks in diametral compression specimens determined by the method of caustics are in agreement with the analytical solutions in the crack length range $a/R = 0.2$ to 0.5 .

3. Fracture toughness of structural ceramics can be assessed at room and elevated temperatures using centre-cracked diametral compression specimens.

4. The chevron-notch geometry and the intrinsic stability of the crack in the diametral compression specimen (i.e. N_1 is a slowly varying function of a/R) ensure initiation and stable propagation of a sharp crack through the chevron notch.

5. For most typical chevron-notch geometries in a diametral compression specimen, the crack instability occurs at the base of the notch (i.e. when $a = a_1$). As a result, fracture toughness is calculated from stress intensity factor solutions for a straight-through crack front and no assumptions are made with respect to the chevron notch.

Acknowledgements

The authors are grateful to Professor Anil V. Virkar for his encouragement and helpful discussions throughout the course of this work. The research was partially supported by the US Department of Energy under Contract No. DEAC0284ER45049.

References

1. O. VARDAR and I. FINNIE, *Int. J. Fract.* **11**(3) (1975) 495.
2. M. C. SHAW, P. M. BRAIDEN and G. J. DE SALVO, *Trans. ASME, J. Eng. Ind.* **97** (1975) 77.
3. S. Ya. YAREMA and G. S. KRESTIN, *Fiz. Khim. Mekh. Mater.* **2** (1) (1966) 10.
4. L. L. LIBATSKII and S. E. KOVCHIK, *Sov. Mater. Sci.* **3** (1967) 334.
5. H. AWAJI and S. SATO, *Trans. ASME, J. Eng. Mater. Tech.* **100**(4) (1978) 175.
6. S. Ya. YAREMA, G. S. IVANITSKAYA, A. L. MAISTRENKO and A. I. ZBOROMIRSKII, *Probl. Proch.* **16**(8) (1984) 51.
7. D. K. SHETTY, A. R. ROSENFELD and W. H. DUCKWORTH, *J. Amer. Ceram. Soc.* **68**(12) (1985) C-325.
8. *Idem*, *Eng. Frac. Mech.* **26** (1987) 825.
9. D. MUNZ, R. T. BUBSEY and J. L. SHANNON Jr, *J. Amer. Ceram. Soc.* **63**(5-6) (1980) 300.
10. D. K. SHETTY, *Trans. ASME, J. Eng. Gas Turb. Power* **109** (1987) 282.
11. C. ATKINSON, R. E. SMELSER and J. SANCHEZ, *Int. J. Fract.* **18**(4) (1982) 279.
12. P. S. THEOCARIS, *J. Appl. Mech.* **37** (1970) 409.
13. P. S. THEOCARIS and E. GDOUTOS, *ibid.* **39** (1972) 91.
14. P. S. THEOCARIS, in "Mechanics of Fracture", Vol. 7, edited by G. C. Sih (Nijhoff, The Hague, 1981) pp. 189-248.
15. G. HONDROS, *Austral. J. Appl. Sci.* **10** (1959) 243.
16. J. E. SRAWLEY, *Int. J. Fract.* **12** (1976) 475.
17. D. G. CARTWRIGHT and D. P. ROOKE, *J. Strain Anal.* **10** (1975) 217.
18. *Idem*, *ibid.* **10** (1975) 259.
19. P. MANOGG, *Glastechn. Ber.* **39** (1966) 323.
20. U. SEIDELMANN, U. SOLTEZ and H. KORDISCH, in "Advances in Research on Strength and Fracture of Materials", edited by D. M. R. Taplin, Vol. 3B (Pergamon, Oxford, 1978) pp. 621-6.
21. T. T. SHIH, *J. Testing Eval.* **9**(1) (1981) 50.
22. WU SHANG-XIAN, *Eng. Fract. Mech.* **19**(2) (1984) 221.
23. J. C. NEWMAN Jr, ASTM STP 855 (American Society for Testing and Materials, Philadelphia, 1984) pp. 5-31.
24. R. F. PABST, K. KROMP and G. POPP, *Proc. Br. Ceram. Soc.* **32** (1982) 89.
25. A. A. SUKERE, *Eng. Fract. Mech.* **26**(1) (1987) 65.
26. R. STREIT and I. FINNIE, *Exp. Mech.* **20**(1) (1980) 17.
27. H. LIEBOWITZ, J. D. LEE and J. EFTIS, *Eng. Fract. Mech.* **10** (1978) 315.
28. J. EFTIS and D. L. JONES, *Int. J. Fract.* **20** (1982) 267.
29. N. A. TRAVITZKY, D. G. BRANDON and E. Y. GUTMANAS, *Mater. Sci. Eng.* **71** (1985) 77.

Received 24 April
and accepted 6 July 1987